RSC Advances

ROYAL SOCIETY OF CHEMISTRY

www.rsc.org/advances

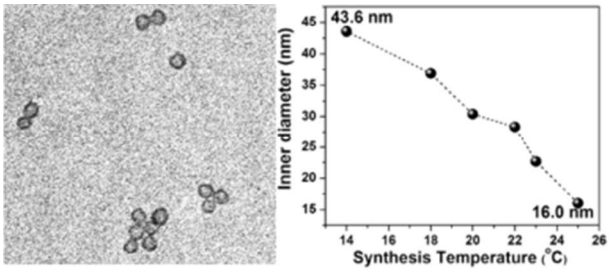

Single-micelle-templated hollow silica nanospheres with inner diameter tunable from 16 to 44 nm were synthesized using Pluronic F108 surfactant and suitable micelle swelling agent through control of initial synthesis temperature

Journal Name

ARTICLE

Single-micelle-templated Synthesis of Hollow Silica Nanospheres with Tunable Pore Structures

Received 00th January 20xx,
Accepted 00th January 20xx

DOI: 10.1039/x0xx00000x

www.rsc.org/

Yingyu Li[a]† and Michal Kruk[a]*

Hollow silica nanospheres (HSNs) were synthesized by using swollen micelles of Pluronic F108 ($EO_{132}PO_{50}EO_{132}$) block copolymer surfactant as soft templates at low silica-precursor/surfactant ratios. An unprecedented tunability of the pore size was achieved in this single-micelle-templating synthesis through the initial synthesis temperature control in F108/toluene system, for which the pore diameter gradually increased from 16 to 44 nm upon decreasing the synthesis temperature from 25 to 14 °C. An additional pore size adjustment coupled with the change in the size of entrances to the nanospheres can be achieved by selecting the hydrothermal treatment temperature, as shown for the synthesis at 25 °C. The inner diameter of the hollow nanospheres can also be modified by changing the silica alkoxide precursor used or its ratio to the surfactant. Moreover, the formation of hollow nanospheres, their inner void size and its temperature adjustability depend on the swelling agent used. In the cases of xylene and ethylbenzene swelling agents, the pore size adjustment was complicated by the morphology change from loose aggregates of hollow spheres to consolidated particles with multiple mesopores as the temperature was lowered. On the other hand, these swelling agents afforded nanospheres of particularly large diameter (22-26 nm) at 25 °C. Less potent swelling agents (1,3,5-triisopropylbenzene and cyclohexane) afforded largely disordered consolidated structures instead of single-micelle-templated nanospheres. The work demonstrated the potential of Pluronic F108 combined with an appropriate swelling agent to template silica nanospheres with hollow interiors of size and accessibility adjustable in a wide range through simple temperature control.

Introduction

Over the last two decades, hollow silica nanospheres (HSNs) have attracted a lot of attention due to their unique properties, such as high specific surface area, large inner void volume, as well as uniform size and inner void diameter.[1-6] These fascinating nanostructures have vast potential applications as catalysts or catalyst supports,[5, 7-11] drug carriers,[12-17] imaging agents,[18] as well as adsorbents and separation materials.[19-23] HSNs are often synthesized using templates that endow the hollow spheres with appropriate (inner) size and are referred to as hard or soft. Hard templates are solid particles, such as polymer latexes (for instance polystyrene or poly(methyl methacrylate) spheres),[1, 24, 25] metal or metal oxide nanoparticles,[26] and poly(N-isopropylacrylamide) aggregates.[27] Silica species are hydrolyzed and condense around the hard templates, which are subsequently removed by calcination, acid etching or solvent extraction. The dimensions of hard templates are fixed and their utility depends on the ability to: (i) prepare them in appropriate sizes, (ii) form the shell on their surfaces and (iii) prevent the aggregation involving the covalent cross-linking. Soft templates that often form through self-assembly of relatively small molecules provide a higher level of flexibility and may be more cost-efficient. They include micelles,[2, 15, 20, 28] vesicles[29, 30] and microemulsions,[31, 32] which can be removed from the nanosphere interiors through calcination or solvent extraction. Micelles are well-known as templates for uniform voids in the frameworks of ordered mesoporous materials (OMMs)[33, 34] and their less well defined counterparts.[35, 36] However, under appropriate conditions, commercially available triblock copolymer surfactants, such as Pluronic F127 ($EO_{106}PO_{70}EO_{106}$) and F108 ($EO_{132}PO_{50}EO_{132}$) (which have been used to template OMMs[34, 37]) interact with silica species to form individual or aggregated HSNs, which are also referred to as single-micelle-templated hollow nanospheres.[2, 20, 38, 39] While the latter can form under different conditions,[2, 3, 15, 20] they tend to be achievable at low ratios of the silica precursor to the block-copolymer surfactant.[37-40] While the details of the single-micelle-templating process may vary, it is considered that a silica precursor (for instance, tetraethyl orthosilicate, TEOS) or its hydrolysis products interact with poly(ethylene oxide) (PEO) blocks in the micelle corona and cross-link therein forming a spherical shell.[18, 41] Additionally, parts of the PEO chains on the periphery of the micelles remain without cover of the silica species and provide a steric stabilization for the

[a] Department of Chemistry, College of Staten Island, City University of New York, 2800 Victory Boulevard, Staten Island, New York 10314 and Graduate Center, City University of New York, 365 Fifth Avenue, New York, New York 10016.
† Present address: Agilent Technologies, 2850 Centerville Rd, Wilmington, DE 19808.
Electronic Supplementary Information (ESI) available: Tables with conditions of the syntheses and with structural parameters derived from SAXS and gas adsorption. Experimental TEM, SAXS and gas adsorption data. See DOI: 10.1039/x0xx00000x

nanoparticles,[18, 41] preventing or limiting the cross-linking between them and thus hindering the formation of consolidated structures, such as ordered mesoporous materials, which would otherwise form.[42]

The nanosphere size and inner void (pore) size control is an important opportunity in single-micelle-templated HSNs, but its practical implementations have been limited. The use of poly(ethylene oxide)-poly(2-vinyl pyridine)-polystyrene (PEO-PVP-PS) surfactants with different sizes of the hydrophobic PS blocks allowed for tuning of the inner size of the hollow spheres from ~10 to ~18 nm.[43] The addition of increasing proportions of polystyrene homopolymer to the micellar system based on a PEO-PVP-PS template led to an increase in the pore diameter of hollow silica spheres from 21 to 27 nm (based on TEM), demonstrating a usefulness of a polymeric swelling agent, but the product was heterogeneous in some cases.[3] The use of different relative amounts of a small-molecule swelling agent in Pluronic F127-based synthesis of organosilicas, which led to a pore diameter increase from ~10 to ~13 nm, also was shown,[20] although its extension to silicas would be beneficial. Another approach was based on the adjustment of the hydrothermal treatment temperature in the synthesis and may generate a limited range of pore diameters.[39] Moreover, the inner void size can be decreased by increasing the calcination temperature.[38] The work on single-micelle-templated organosilica nanospheres suggests that the use of different swelling agents may also allow for the adjustment of the inner sphere diameter.[38] The tuning of the size of entrances to the nanospheres is another important ability and it was achieved recently by using different temperatures of the hydrothermal treatment.[39]

Though HSNs with well-defined structures and uniform particle sizes have been reported as discussed above, the development of a methodology for the fabrication of HSNs with easily tunable size of inner spherical voids would be highly desirable. Moreover, the understanding of the factors that influence the formation of hollow nanospheres is still at its early stage. Herein,[44] it is demonstrated that in the presence of micelle swelling agents, one can use the initial synthesis temperature adjustment strategy, demonstrated earlier for ordered mesoporous materials,[45, 46] to generate hollow silica nanospheres with widely tunable sizes. However, the adjustment may be complicated by a transition from individual or aggregated hollow nanoparticles to consolidated materials as temperature decreases. Moreover, the effect of the use of different swelling agents was studied and as a result, the synthesis of hollow nanospheres with very large interiors at room temperature was developed. The effect of hydrothermal treatment temperature was also studied. In this work,[44] Pluronic F108 ($EO_{132}PO_{50}EO_{132}$) with a larger hydrophilic blocks was selected as a surfactant.

Experimental

Synthesis

Pluronic F108 ($EO_{132}PO_{50}EO_{132}$) was provided by BASF as a research sample. Ethylbenzene, toluene (extra dry), and *m*-xylene were obtained from Fisher Scientific. 1,3,5-triisopropylbenzene (TIPB) was acquired from Alfa Aesar. Tetraethyl orthosilicate (TEOS), tetramethyl orthosilicate (TMOS) and cyclohexane were purchased from Acros. All of these chemicals were used directly without further purification. In a typical synthesis of hollow silica nanospheres, 1.00 g of Pluronic F108 was added to 60 mL of 2 M HCl solution, which was followed by magnetic stirring until the copolymer surfactant dispersed at a selected temperature (12-25 °C). Next, a selected volume of a swelling agent (for instance, 3 mL of toluene or 3.46 mL of *m*-xylene or 3.44 mL of ethylbenzene) was added and the stirring continued in a covered container. After 30 min, silica precursor TEOS (or TMOS) was added. The reaction mixture continued to stir at 350 rpm for 1 day. Then the reaction mixture was treated hydrothermally at 100 °C for 1 day in a closed polypropylene bottle. The resulting as-synthesized sample was filtered, washed with deionized water and dried at ~ 60 °C in a vacuum oven. Finally, the sample was calcined at 550 °C under air for 5 h (heating ramp 2 °C/min). The samples are denoted HSNx, where HSN stands for hollow silica nanosphere, and x is the sample number. The synthesis conditions of HSNs are summarized in Supporting Table S1. It should be noted that some samples from this series may actually not exhibit hollow sphere morphology, even though the conditions were selected to be favorable for the hollow sphere formation.

Characterization

Small-angle X-ray scattering (SAXS) patterns were recorded on a Bruker Nanostar U instrument equipped with a rotating anode Cu K_α radiation source operated at 50 kV, 24 mA and with Vantec 2000 2-dimensional detector. Samples were placed in the hole of an aluminium sample holder and secured on both sides using a Kapton tape. Nitrogen adsorption measurements were performed at -196 °C on a Micromeritics ASAP 2020 volumetric adsorption analyzer. Before the analysis, the silica samples were outgassed under vacuum at 200 °C for 2 h in the port of the adsorption analyzer. Transmission electron microscopy (TEM) images were acquired on a FEI Tecnai Spirit microscope operated at 120 kV. TEM images for HSNs prepared using ethylbenzene as a swelling agent were obtained on a Hitachi H-800 microscope operated at 100 kV. Before the imaging, the samples were dispersed in ethanol using sonication and deposited on a carbon-coated copper grid after which the solvent was evaporated under air. The BET specific surface area[47] (S_{BET}) was calculated from the nitrogen adsorption isotherm in a relative pressure range from 0.04 to 0.20. Total pore volume (V_t) was determined from the amount adsorbed at a relative pressure of 0.99.[47] Pore size distributions (PSDs) were determined from adsorption branches of the isotherms using the Barrett-Joyner-Halenda (BJH) method with KJS correction[48] for cylindrical mesopores and the statistical film thickness curve for a macroporous silica gel LiChrospher Si-1000.[49] This method is known to underestimate the diameter of spherical mesopores of

ordered mesoporous silicas by 2-4 nm in the considered pore size range.[50]

Results and discussion

Effect of initial synthesis temperature

In most of the experiments, the molar ratio of TEOS to Pluronic F108 was low (99:1)[38] to facilitate the formation of single-micelle-templated nanoparticles instead of consolidated structures. When toluene was used as a swelling agent, hollow nanospheres (sample HSN01; see TEM in Figure 1) with a very large inner diameter (~44 nm based on gas adsorption; see Figure 2, Supporting Figure S1 and Table S2) formed at the initial synthesis temperature of 14 °C with subsequent hydrothermal treatment at 100 °C. However, the nanospheres were not uniform in size, as seen from TEM and the pore size distribution (Supporting Figure S1).

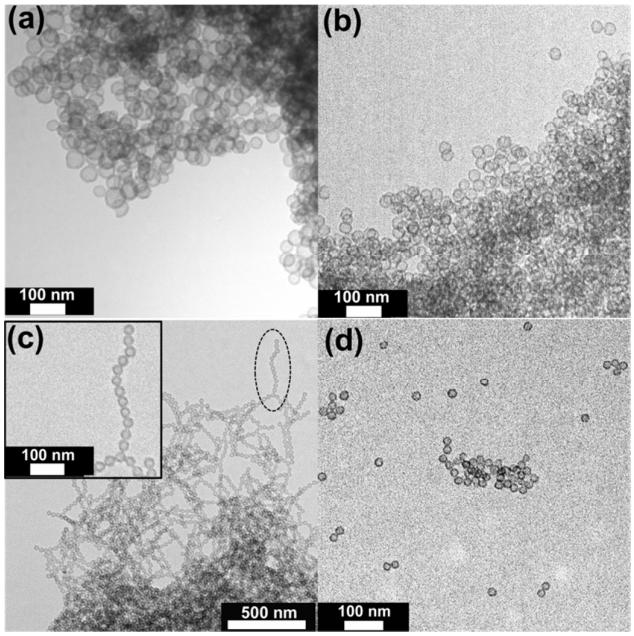

Figure 1. Transmission electron microscopy images of hollow silica nanospheres synthesized at different temperatures: (a) 14 °C (HSN01), (b) 22 °C (NSN04), (c) 25°C for as-synthesized sample (HSN06), and (d) calcined HSN06. Taken in part from Ref.[44]

The above inner void diameter was very large as for single-micelle-templated nanoparticles. It was larger than the pore diameter of silica nanospheres templated by Pluronic F127/toluene pair (36 nm in the case of a comparable hydrothermal treatment)[39] and larger than that attained with Pluronic F108/xylene pair in the presence of an inorganic salt (KCl).[38] While Pluronic F108 ($EO_{132}PO_{50}EO_{132}$) has a larger molecular weight than Pluronic F127 ($EO_{106}PO_{70}EO_{106}$), the hydrophobic block size of the former is appreciably smaller (50 vs. 70 repeating units on average). In both cases, the fully extended hydrophobic block length (on average about 20 and 28 nm, respectively) was not enough to span over the entire pore diameter, which suggests that the inner parts of the cores of swollen micelles were filled with a swelling agent and devoid of PPO blocks. This in turn suggests that the template for the formation of the hollow nanospheres can be considered either as a swollen micelle or a stabilized microemulsion droplet. At first, it may appear that the stabilized microemulsion nature may be a source of the polydispersity of the considered hollow spheres. However, microemulsion templates may be quite uniform in size.[31, 51] Moreover, as can be seen below, quite large nanospheres can be obtained with a much more narrow pore size distribution.

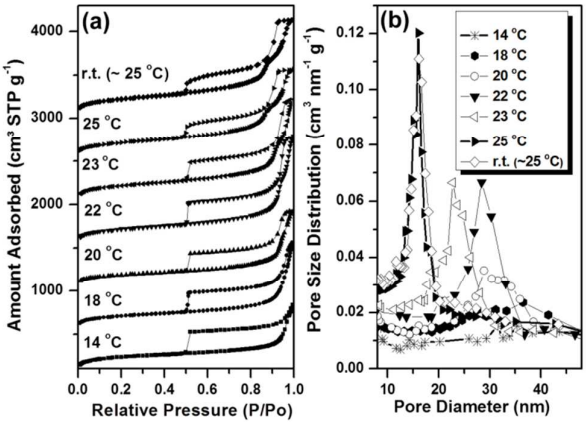

Figure 2. (a) Nitrogen adsorption isotherms and (b) pore size distributions (data for samples prepared at 14, 18 and 20 °C are also shown in Supporting Figure S1) for calcined hollow silica nanospheres synthesized with Pluronic F108/toluene pair at different temperatures.[44]

While a decrease in initial synthesis temperature to 12 °C rendered mostly consolidated structures instead of hollow nanosphere products, an increase in temperature did not disrupt the nanosphere morphology. As the temperature was increased to 18 °C, the pore diameter of the sample (HSN02) became more uniform, but decreased, while being still as large as ~37 nm (Figure 2 and Supporting Figure S1). At 20 °C, the pore size decreased to ~30 nm. Around room temperature (22 and 23 °C), the pore diameter became even more uniform and was 23-28 nm and TEM confirmed the well-defined hollow nanosphere morphology (Figure 1(b)). The formation of hollow nanospheres with fairly large mesopore interiors was also possible at 25 °C (see Figure 1(c, d)). The pore diameter calculated from the N_2 adsorption isotherm was ~16 nm. The BET specific surface area was 761 m^2 g^{-1} and the total pore volume was 1.65 cm^3 g^{-1} (Supporting Table S2). It is also noteworthy that when the synthesis was carried out at room temperature (~25 °C) without the temperature control, the pore diameter of the resulting sample (HSN07) was comparable to that of the sample (HSN06) prepared at 25 °C with accurate temperature control (Figure 2).

As seen in Figure 2, the considered samples (except for the sample prepared at 14 °C) exhibited adsorption isotherms with two more or less separated hysteresis loops at relative pressures between 0.5 and 0.85-0.95 as well as between ~0.9 and 1, suggesting that these samples have two types of mesopores: quite uniform voids inside the particles and less well defined pores attributable to interparticle voids arising

from a loose packing of the nanospheres (Figure 1). In the case of the sample prepared at 14 °C, the large sphere size might have resulted in large interparticle void size, and consequently, in the limited capillary condensation very close to the saturation vapor pressure. The capillary evaporation from the uniform mesopores was delayed to the lower limit of adsorption-desorption hysteresis (P/P_o = 0.4-0.5), indicating that the gaps in the walls that provide the access to the sphere interiors were of diameter below 5 nm.[52] Only the samples prepared at ~25 °C exhibited capillary evaporations from their uniform mesopores commencing above the lower limit of hysteresis, indicating the presence of gaps above 5 nm in diameter[52] in the shells of some nanospheres. It should be noted that the above size estimates are based on several assumptions. The shape of the gaps is assumed to be approximately circular, while it is actually likely to be irregular based on TEM observation of single-micelle-templated nanospheres.[39] It is also assumed that the adsorption-desorption behavior of the pores (gaps) in the shell of the nanoparticles is similar to the behavior of long cylindrical mesopores, even though the thickness of the wall and thus the "length" of the pore in the shell is comparable to its diameter. This is certainly an approximation, because pores of low length/width ratio are known to exhibit a capillary condensation and evaporation at somewhat higher pressures than their longer counterparts of the same width.[53] Another assumption is that the desorption behavior from the nanosphere interior is similar to that from mesopores within an ordered mesoporous material with multiple mesopores separated by walls. The validity of these assumptions is uncertain. Still, the capillary evaporation pressure is expected to reflect the sizes of the openings in the shell, which are difficult to quantify even if they are observable by TEM.

When toluene was used as a micelle swelling agent in the 14-25 °C range of initial synthesis temperatures, the single-micelle-templated mesopores were of diameter 16-44 nm, which increased as the initial synthesis temperature decreased, as discussed above. These results show for the first time that the inner diameter of single-micelle-templated nanospheres (prepared in the presence of a swelling agent) can be tuned systematically and in a wide range through the initial synthesis temperature control. Earlier studies showed that lower temperature in the sub-ambient range allows one to achieve larger pore sizes in the swelling-agent-assisted syntheses of Pluronic-templated ordered silicas with spherical[39, 45, 54] and cylindrical[46] mesopores, but these were consolidated structures templated by multiple micelles rather that single-micelle-templated nanoparticles. In fact, the above temperature dependence of the pore size was somewhat different from the dependence observed for FDU-12 templated by Pluronic F108/toluene pair used herein.[42] A sharp pore size increase was observed for FDU-12 in 23-28 °C range as the temperature decreased, followed by a range in which the pore size was largely temperature-independent. Herein, the pore size increase was particularly large in 22-25 °C range, which is similar, but further gradual pore size increase was seen as temperature was lowered to 14 °C. Moreover, as is shown hereafter, other Pluronic F108/swelling-agent pairs may exhibit the temperature dependence of the pore size that is obscured by a transition from single-micelle-templated nanoparticles to consolidated structures as the initial synthesis temperature is decreased.

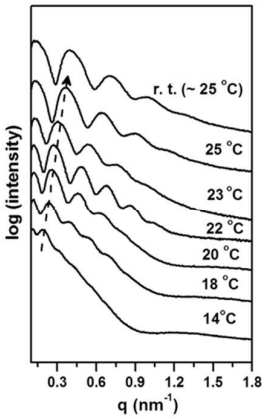

Figure 3. SAXS patterns of hollow silica nanospheres prepared at different initial temperatures using Pluronic F108/toluene pair as the template with the hydrothermal treatment at 100 °C.[44]

Figure 1(c) shows that as-synthesized sample prepared at 25 °C (HSN06) was apparently composed of chains of hollow spherical nanoparticles, but after calcination, this morphology was disrupted and broken down into individual hollow silica nanospheres, short chains of beads, or aggregates (Figure 1(d) and Supporting Figure S2). Similar, but less profound, morphological changes were also seen after extraction. These observations suggest that some structures of single-micelle-templated nanoparticles may be so fragile that it may be difficult to preserve them during the surfactant removal.

The temperature increase resulted in a systematic shift of the position of peaks on SAXS patterns to higher angles (Figure 3), as expected on the basis of the pore size changes and the corresponding diameter changes for the sphere products. The patterns featured multiple broad peaks and resembled the ones reported earlier for (aggregated) hollow nanospheres.[38, 39, 55, 56] Based on earlier studies of scattering of micelles,[56] it appears that the considered SAXS patterns are primarily determined by the form factor for hollow spheres with strongly scattering shell. The pattern for the sample prepared at 14 °C was less well resolved, which may be related to a higher size dispersity of the nanospheres present in this sample.

Effect of the swelling agent

A variety of organic compounds are known to successfully serve as micelle swelling agents, including benzene and its alkyl-substituted derivatives,[33, 34, 37, 46] linear hydrocarbons,[57, 58] cyclic hydrocarbons,[46, 59] and long-chain amines.[60] Even though these compounds are known primarily from their pore enlarging action, they may in some cases serve a more profound role of additives that allow for the formation of the micelle-templated structure.[61] As seen in Figure 4, in the absence of a swelling agent at 25 °C, a silica sample was

obtained that exhibited no clear capillary condensation step on its gas adsorption isotherm. This behavior suggests the lack of micelle-templated mesopores, even if single surfactant molecules may be embedded in the silica framework and may template (micro)porosity.[61]

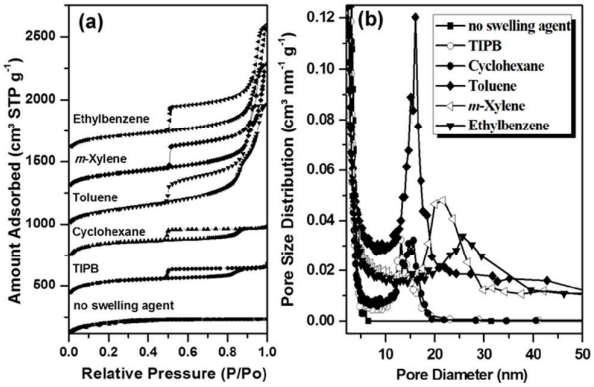

Figure 4. (a) Nitrogen adsorption isotherms, and (b) pore size distributions for calcined silica samples synthesized at 25 °C in the absence of swelling agent and in the presence of different swelling agents.[44]

In the presence of a swelling agent, the outcome depended in a fairly systematic way on the swelling agent used. When moderate swelling agents, such as 1,3,5-triisopropylbenzene (TIPB) or cyclohexane,[46, 61] were employed, the resulting samples displayed nitrogen adsorption isotherms with a single capillary condensation step (Figure 4), suggesting that their structures were consolidated instead of being composed of separate single-micelle-templated silica particles, which was confirmed through TEM observation (Supporting Figure S3). Interestingly enough, the increase in the volume of TIPB did not result in any appreciable increase in the pore diameter (Supporting Figure S4), suggesting that the use of about 3 mL TIPB per 1 g of Pluronic F108 surfactant can fully saturate the micelles of the block copolymer. However, it is not clear why moderately strong swelling agents would promote the formation of consolidated structures instead of hollow nanospheres. Perhaps a stronger swelling promotes a hard-sphere behavior[37] and thus limits the cross-linking and leads to the preservation of identifiable single-micelle-templated building blocks in the material, while less swollen hybrid silica/micelle building blocks distort and consolidate more readily.

At 25 °C, more potent swelling agents, such as toluene, *m*-xylene, or ethylbenzene, generated single-micelle-templated nanoparticles with inner pore voids of diameter from 16 to 26 nm (Supporting Tables S3 and S4). The influence of the initial synthesis temperature on the pore size of the obtained materials is shown in Figure 5. As discussed above, HSNs with the inner pore size of 16-44 nm can be synthesized using Pluronic F108/toluene pair. It is notable that at or near room temperature (25 °C), Pluronic F108/toluene pair renders surprisingly small mesopore cavity, when compared with F108/ethylbenzene pair that provided the largest pore diameter of 26 nm, followed by F108/*m*-xylene pair (Figures 4 and 5; Supporting Tables S3 and S4).

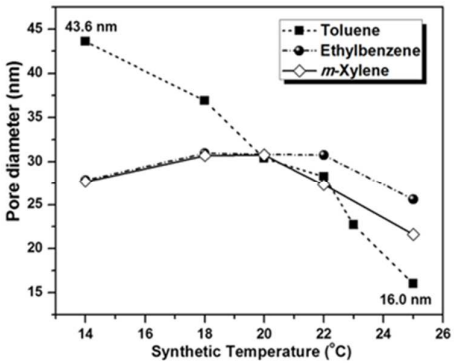

Figure 5. Inner pore diameter (from gas adsorption) as a function of the initial synthesis temperature for calcined silicas prepared using different swelling agents. The lines serve to guide the eye. Taken from Ref.[44] with modification.

For F108/ethylbenzene and F108/m-xylene templating pairs, the pore size increased as the temperature decreased, as in the case of F108/toluene pair, until the temperature of ~20 °C was reached, below which the pore size decreased to some extent. At the same time, the position of the first peak on the SAXS pattern continued shifting to lower angles as the temperature decreased, and the peaks became more narrow at 18 °C or lower (Figure 6 and Supporting Figure S5). In the case of the Pluronic F108/ethylbenzene pair, the samples formed highly aggregated (18 °C) or fully consolidated (14 °C) structures with spherical mesopores instead of loose aggregates of hollow nanoparticles (see TEM in Figure 7). Apparently, as the temperature was lowered, a tendency to form consolidated structures became stronger. This is consistent with an earlier finding that a consolidated periodic structure composed of hollow spherical building blocks was obtained at 20 °C for Pluronic F108/1,3,5-trimethylbenzene pair, whereas loose aggregates of single-micelle-templated nanoparticles were recovered at 30 °C.[37] In the aforementioned study, an inorganic salt was present in the synthesis mixture, unlike in the present case. Still, our results indicate that the earlier finding reflects a general behavior and additionally suggest that the temperature at which the change from the consolidated structures to individual (or loosely aggregated) single-micelle-templated nanoparticles takes place depends on the kind of the swelling agent used. The fact that toluene behaved differently from xylene and ethylbenzene is not surprising, as the latter two were shown to have a similar performance as swelling agents in the synthesis of ordered mesoporous silicas and organosilicas,[62, 63] while toluene had a somewhat different action.[39, 61] It is also clear that the departure from the trend of increasing the pore diameter as the temperature decreases coincided with the change from a single-micelle-templated structure to a consolidated (or highly aggregated) structure. Still, it is not clear what triggered the departure from the pore size trend. The inspection of nitrogen adsorption isotherms reveals the decrease in the height of the capillary condensation step (and thus in the mesopore volume) for samples prepared at either 14 °C (ethylbenzene) or 18 °C (m-xylene). The decrease in the mesopore volume may result in the pore size decrease even if

the repeating distances are comparable or somewhat larger, because the lower mesopore volume is likely to result from a larger pore wall thickness.

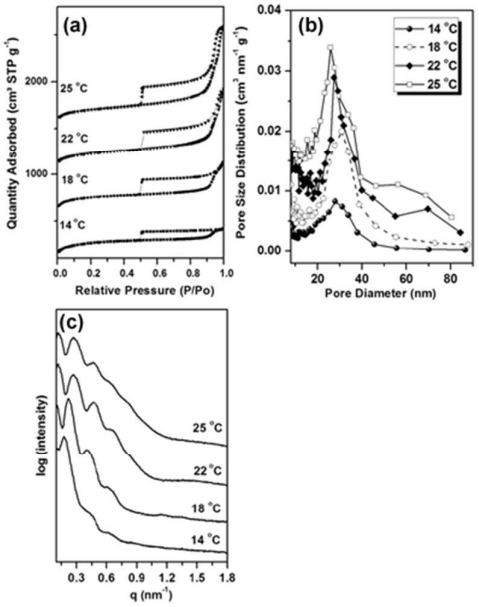

Figure 6. (a) Nitrogen adsorption isotherms, (b) pore size distributions and (c) SAXS patterns for calcined silicas prepared at different initial temperatures using F108/ethylbenzene pair.[44]

Moreover, the repeating distances for the different samples discussed herein may not necessarily be directly comparable, as broad maxima of SAXS patterns for somewhat aggregated single-micelle-templated nanoparticles have a different meaning[55] than the narrower peaks of consolidated and periodic (or weakly periodic) structures. As mentioned above, the SAXS patterns for the nanoparticles seem to reflect primarily the form factor for hollow spheres, while those of ordered mesoporous materials reflect the structure factor[55] dependent on the arrangement of the structural units in space.

As for the consolidation into multi-pore nanoparticles or the preservation of single-micelle-templated nanoparticles, multiple factors may contribute. At higher temperature, the thermal motion of nanoparticles in solution is faster, so is the formation of siloxane crosslinks through silanol condensation.[37] Perhaps faster moving and cross-linking hybrid silica/micelle nanoparticles more easily form a limited number of cross-links that are not easily restructured, thus preventing an efficient aggregation (potentially followed by a consolidation).

Effect of framework precursor

The samples discussed above were prepared using tetraethyl orthosilicate (TEOS) with TEOS:Pluronic F108 molar ratio of 99:1. When the TEOS:F108 molar ratio was increased to 145:1 at 25 °C (HSN13) in the synthesis involving toluene, well-defined HSNs were obtained with uniform pore diameter of ~18 nm, which is a little larger than those obtained with 99:1 ratio. When tetramethyl orthosilicate (TMOS) known from faster hydrolysis and condensation was selected as a silica source instead of TEOS (TMOS:Pluronic F108 = 99:1), well-defined HSNs (sample HSN14) prepared using Pluronic F108/toluene pair were also successfully synthesized (Supporting Figure S6). The material had the BET specific surface area of 757 m^2 g^{-1}, and a narrow pore size distribution centered at as much as 21 nm (Supporting Figure S7, and Table S5).

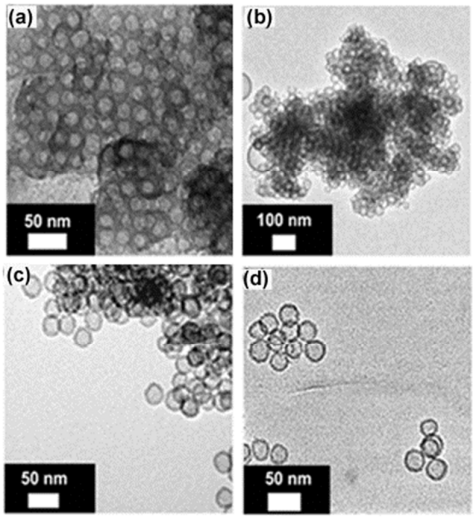

Figure 7. TEM images of calcined silica samples synthesized using F108/ethylbenzene pair at different temperatures: (a) 14, (b) 18, (c) 22 and (d) 25 °C.[44] Note that samples recovered after nitrogen adsorption measurements were imaged.

Effect of the hydrothermal treatment temperature

Besides the initial synthesis temperature, the hydrothermal treatment temperature also plays a role in controlling the pore size of the hollow nanospheres, as shown in our earlier work for treatments at 100-140 °C.[39] Herein, a wider temperature range was explored. At the initial temperature of 25 °C, the product obtained without hydrothermal treatment passed through the filter. Therefore, a part of the synthesis mixture was dialyzed at room temperature, filtered, and lyophilized into a white powder. The TEM image revealed chains of connected hollow spheres (Supporting Figure S8(a)). After removal of the surfactant via calcination, the pore diameter was around 10 nm. Huo and co-workers[41] prepared silica cross-linked micelles without a hydrothermal treatment using Pluronic F127, and a particle size of ~10 nm was measured by cryo-TEM. After appropriate stabilization, the particles would not settle in the solution. So our result is not surprising in the light of this earlier work in which no swelling agent was used. When another portion of the synthesis mixture was hydrothermally treated at 60 or 80 °C, as-synthesized samples isolated by filtration contained individual HSNs and chains of beads, but the particle size was not uniform, as seen from TEM (Supporting Figure S8). The adsorption isotherms of these samples (Figure 8) leveled off after the capillary condensation at a relative pressure of ~0.8, and thus were different from the isotherms discussed above in the context of single-micelle-templated hollow nanospheres. However, SAXS patterns of all calcined samples exhibited a background at low angles that

was similar to that seen for single-micelle-templated nanoparticles (although less intense) (Supporting Figure S9).

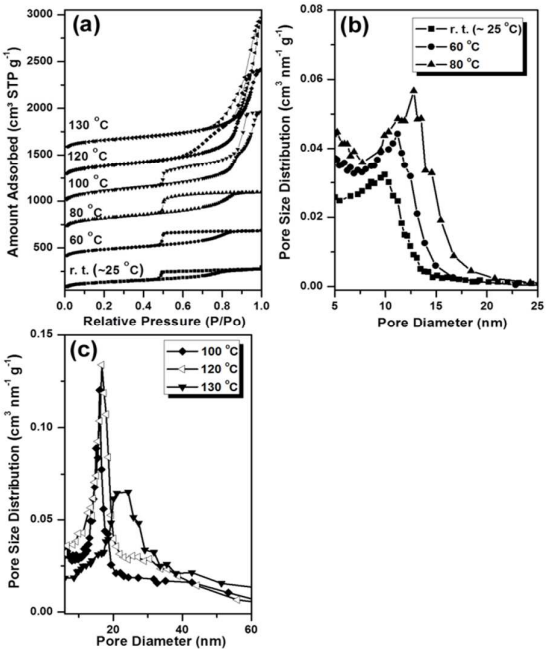

Figure 8. (a) Nitrogen adsorption isotherms and (b,c) pore size distributions for calcined silicas prepared at 25 °C using Pluronic F108/toluene pair with hydrothermal treatments at different temperatures. Taken in part from Ref.[44]

In conjunction with TEM images discussed above, the SAXS data suggest that these are not consolidated materials in a sense considered above. Rather, these are likely to be compact aggregates of single-micelle-templated nanoparticles, in which the size of voids between the building blocks is comparable to the size of the hollow interiors, leading to a broad pore size distribution based on contributions from the two groups of mesopores. This would explain the observation that pore size distributions of these samples were much broader than those of the samples hydrothermally treated at higher temperatures (100 °C or higher).

It is not fully clear what triggers the apparent change from compact aggregates to loose aggregates (or individual nanospheres). Perhaps a higher hydrothermal treatment temperature leads to more extensive cross-linking into loose structures with low number of nearest neighbors per sphere, whereas the samples that did not undergo such a treatment exhibit a higher mobility of the hybrid micelles and thus can more readily pack into quite compact aggregates.

It is noteworthy that with the help of the hydrothermal treatment at different temperatures, the HSNs with hollow interiors of diameter up to 23 nm (7 nm above the pore diameter in the case of the treatment at 100 °C that is mostly discussed herein) can be obtained, which increased as the treatment temperature increased (Figure 8 and Supporting Table S6). This is consistent with our earlier results. In addition, when the hydrothermal treatment was carried out at 120-130 °C, the hysteresis loops no longer extended to the lower limit of adsorption-desorption hysteresis (relative pressure of 0.4-0.5), but were much more narrow. This provides an evidence of the increase of the size of entrances (gaps) in the shell of the nanospheres and is consistent with the results of our earlier work.[39] Since the capillary evaporation was observed at a relative pressure of ~0.7 or higher, one can infer that the diameters of the entrances in the shells are on the order of 10 nm.

Conclusions

The single-micelle-templating method allowed us to synthesize well-defined hollow silica nanospheres using a low precursor/surfactant ratio at room temperature. The inner spherical void diameter can be tailored in a wide range from 16 nm to ~44 nm by adjusting the initial synthesis temperature in the presence of a swelling agent. Additionally, the hydrothermal treatment temperature can be used to tune the inner void size and its accessibility. The pore size may also be dependent on the silica precursor used and its ratio to the surfactant. However, as the initial synthesis temperature decreases, a transition from the hollow nanosphere morphology to a consolidated (perhaps disordered) morphology may be observed. Moreover, swelling agents that solubilize less in Pluronics may afford consolidated structures instead of hollow nanospheres under conditions at which the "stronger" swelling agents readily generate the nanospheres. The discussed synthetic strategy provides a convenient avenue to hollow spherical silica nanoparticles with widely adjustable cavity size and accessibility. and pore

Acknowledgements

NSF is gratefully acknowledged for partial support of this research (awards DMR-0907487 and DMR-1310260) and for funding the acquisition of SAXS/WAXS system through award CHE-0723028. Acknowledgment is made to the Donors of the American Chemical Society Petroleum Research Fund for partial support of this research (Award PRF #49093-DNI5). The Imaging Facility at CSI is acknowledged for providing access to TEM. Dr. Zengyan Wei, Hunter College, is gratefully acknowledged for help in some TEM imaging. BASF is acknowledged for the donation of the Pluronic block copolymers. Professor Shuiqin Zhou, CSI, is gratefully acknowledged to helpful discussions.

Notes and references

1. F. Caruso, R. A. Caruso and H. Moehwald, *Science*, 1998, **282**, 1111-1114.
2. J. Tang, J. Liu, P. Wang, H. Zhong and Q. Yang, *Microporous Mesoporous Mater.*, 2010, **127**, 119-125.
3. D. Liu, M. Sasidharan and K. Nakashima, *J. Colloid Interface Sci.*, 2011, **358**, 354-359.
4. S.-H. Wu, C.-Y. Mou and H.-P. Lin, *Chem. Soc. Rev.*, 2013, **42**, 3862-3875.

5. X. Li, Y. Yang and Q. Yang, *J. Mater. Chem. A*, 2013, **1**, 1525-1535.
6. Y. Zhang, B. Y. W. Hsu, C. Ren, X. Li and J. Wang, *Chem. Soc. Rev.*, 2015, **44**, 315-335.
7. Q. Zhang, X.-Z. Shu, J. M. Lucas, F. D. Toste, G. A. Somorjai and A. P. Alivisatos, *Nano Lett.*, 2014, **14**, 379-383.
8. P. Wang, S. Bai, J. Zhao, P. Su, Q. Yang and C. Li, *ChemSusChem*, 2012, **5**, 2390-2396.
9. J. Gao, J. Liu, J. Tang, D. Jiang, B. Li and Q. Yang, *Chem. Eur. J.*, 2010, **16**, 7852-7858.
10. J. Gao, J. Liu, S. Bai, P. Wang, H. Zhong, Q. Yang and C. Li, *J. Mater. Chem.*, 2009, **19**, 8580-8588.
11. J. Gao, X. Zhang, Y. Lu, S. Liu and J. Liu, *Chem. Eur. J.*, 2015, **21**, 7403–7407.
12. A. Corma, U. Díaz, M. Arrica, E. Fernández and Í. Ortega, *Angew. Chem. Int. Ed.*, 2009, **48**, 6247-6250.
13. J. Zhang, S. Karmakar, M. Yu, N. Mitter, J. Zou and C. Yu, *Small*, 2014, **10**, 5068–5076.
14. T. Wang, F. Chai, Q. Fu, L. Zhang, H. Liu, L. Li, Y. Liao, Z. Su, C. Wang, B. Duan and D. Ren, *J. Mater. Chem.*, 2011, **21**, 5299-5306.
15. J. Zhu, J. Tang, L. Zhao, X. Zhou, Y. Wang and C. Yu, *Small*, 2010, **6**, 276-282.
16. W. Yang and B. Li, *J. Mater. Chem. B*, 2013, **1**, 2525-2532.
17. S. K. Das, M. K. Bhunia, D. Chakraborty, A. R. Khuda-Bukhsh and A. Bhaumik, *Chem. Commun.*, 2012, **48**, 2891-2893.
18. H. Tan, N. S. Liu, B. He, S. Y. Wong, Z.-K. Chen, X. Li and J. Wang, *Chem. Commun.*, 2009, 6240-6242.
19. M. Najafi, Y. Yousefi and A. A. Rafati, *Separation and Purification Technology*, 2012, **85**, 193-205.
20. N. Hao, H. Wang, P. A. Webley and D. Zhao, *Microporous Mesoporous Mater.*, 2010, **132**, 543-551.
21. S. Bai, J. Liu, J. Gao, Q. Yang and C. Li, *Microporous Mesoporous Mater.*, 2012, **151**, 474-480.
22. L. Zhang, S. Wu, C. Li and Q. Yang, *Chem. Commun.*, 2012, **48**, 4190-4192.
23. H. Wang, M. Tang, L. Han, J. Cao, Z. Zhang, W. Huang, R. Chen and C. Yu, *J. Mater. Chem. A*, 2014, **2**, 19298-19307.
24. Y. Wan and S.-H. Yu, *J. Phys. Chem. C*, 2008, **112**, 3641-3647.
25. M. Chen, L. Wu, S. Zhou and B. You, *Adv. Mater.*, 2006, **18**, 801-806.
26. J. Liu, S. Z. Qiao, S. B. Hartono and G. Q. Lu, *Angew. Chem. Int. Ed.*, 2010, **49**, 4981-4985.
27. B. Du, Z. Cao, Z. Li, A. Mei, X. Zhang, J. Nie, J. Xu and Z. Fan, *Langmuir*, 2009, **25**, 12367-12373.
28. J.-J. Yuan, O. O. Mykhaylyk, A. J. Ryan and S. P. Armes, *J. Am. Chem. Soc.*, 2007, **129**, 1717-1723.
29. H. Wang, Y. Wang, X. Zhou, L. Zhou, J. Tang, J. Lei and C. Yu, *Adv. Funct. Mater.*, 2007, **17**, 613-617.
30. Y.-Q. Yeh, B.-C. Chen, H.-P. Lin and C.-Y. Tang, *Langmuir*, 2006, **22**, 6-9.
31. Y.-S. Lin, S.-H. Wu, C.-T. Tseng, Y. Hung, C. Chang and C.-Y. Mou, *Chem. Commun.*, 2009, 3542-3544.
32. C.-H. Lin, J.-H. Chang, Y.-Q. Yeh, S.-H. Wu, Y.-H. Liu and C.-Y. Mou, *Nanoscale*, 2015, **7**, 9614-9626.
33. J. S. Beck, J. C. Vartuli, W. J. Roth, M. E. Leonowicz, C. T. Kresge, K. D. Schmitt, C. T. W. Chu, D. H. Olson, E. W. Sheppard, S. B. McCullen, J. B. Higgins and J. L. Schlenker, *J. Am. Chem. Soc.*, 1992, **114**, 10834-10843.
34. D. Zhao, Q. Huo, J. Feng, B. F. Chmelka and G. D. Stucky, *J. Am. Chem. Soc.*, 1998, **120**, 6024-6036.
35. S. A. Bagshaw, E. Prouzet and T. J. Pinnavaia, *Science*, 1995, **269**, 1242-1244.
36. P. T. Tanev and T. J. Pinnavaia, *Science*, 1995, **267**, 865-867.
37. J. Tang, X. Zhou, D. Zhao, G. Q. Lu, J. Zou and C. Yu, *J. Am. Chem. Soc.*, 2007, **129**, 9044-9048.
38. M. Mandal and M. Kruk, *Chem. Mater.*, 2012, **24**, 123-132.
39. L. Huang and M. Kruk, *Chem. Mater.*, 2015, **27**, 679–689.
40. A. Khanal, Y. Inoue, M. Yada and K. Nakashima, *J. Am. Chem. Soc.*, 2007, **129**, 1534-1535.
41. Q. Huo, J. Liu, L.-Q. Wang, Y. Jiang, T. N. Lambert and E. Fang, *J. Am. Chem. Soc.*, 2006, **128**, 6447-6453.
42. Y. Li, J. Yi and M. Kruk, *Chem. Eur. J.*, 2015, **DOI: 10.1002/chem.201500189**.
43. D. Liu, A. Khanal, K. Nakashima, Y. Inoue and M. Yada, *Chem. Lett.*, 2009, **38**, 130-131.
44. Y. Li, Ph.D. Dissertation, City University of New York, 2014.
45. J. Fan, C. Yu, J. Lei, Q. Zhang, T. Li, B. Tu, W. Zhou and D. Zhao, *J. Am. Chem. Soc.*, 2005, **127**, 10794-10795.
46. L. Cao, T. Man and M. Kruk, *Chem. Mater.*, 2009, **21**, 1144-1153.
47. K. S. W. Sing, D. H. Everett, R. A. W. Haul, L. Moscou, R. A. Pierotti, J. Rouquerol and T. Siemieniewska, *Pure Appl. Chem.*, 1985, **57**, 603-619.
48. M. Kruk, M. Jaroniec and A. Sayari, *Langmuir*, 1997, **13**, 6267-6273.
49. M. Jaroniec, M. Kruk and J. P. Olivier, *Langmuir*, 1999, **15**, 5410-5413.
50. M. Kruk and C. M. Hui, *Microporous Mesoporous Mater.*, 2008, **114**, 64-73.
51. A. Imhof and D. J. Pine, *Nature*, 1997, **389**, 948-951.
52. M. Kruk and M. Jaroniec, *Chem. Mater.*, 2003, **15**, 2942-2949.
53. W. J. Stroud, J. E. Curry and J. H. Cushman, *Langmuir*, 2001, **17**, 688-698.
54. G. Ma, X. Yan, Y. Li, L. Xiao, Z. Huang, Y. Lu and J. Fan, *J. Am. Chem. Soc.*, 2010, **132**, 9596-9597.
55. Z. H. Chen, C. Kim, X.-b. Zeng, S. H. Hwang, J. Jang and G. Ungar, *Langmuir*, 2012, **28**, 15350-15361.
56. J. S. Pedersen and M. C. Gerstenberg, *Macromolecules*, 1996, **29**, 1363-1365.
57. P. Feng, X. Bu, G. D. Stucky and D. J. Pine, *J. Am. Chem. Soc.*, 2000, **122**, 994-995.
58. J. Sun, H. Zhang, D. Ma, Y. Chen, X. Bao, A. Klein-Hoffmann, N. Pfaender and D. S. Su, *Chem. Commun.*, 2005, 5343-5345.
59. M. Mandal and M. Kruk, *J. Mater. Chem.*, 2010, **20**, 7506-7516.
60. A. Sayari, Y. Yang, M. Kruk and M. Jaroniec, *J. Phys. Chem. B*, 1999, **103**, 3651-3658.
61. M. Mandal and M. Kruk, *J. Phys. Chem. C*, 2010, **114**, 20091-20099.
62. L. Huang and M. Kruk, *J. Colloid Interface Sci.*, 2012, **365**, 137-142.

63. M. Mandal and M. Kruk, *Z. Anorg. Allg. Chem.*, 2014, **640**, 624-631.